

Inhomogeneous Elastic Response of Silica Glass

F. Léonforte,¹ A. Tanguy,¹ J. P. Wittmer,² and J.-L. Barrat¹

¹Laboratoire de Physique de la Matière Condensée et des Nanostructures Université Lyon I; CNRS, UMR 5586, 43 Boulevard du 11 Novembre 1918, 69622 Villeurbanne Cedex, France

²Institut Charles Sadron, CNRS, 6, Rue Boussingault, 67083 Strasbourg, France
(Received 15 December 2005; published 31 July 2006)

Using large scale molecular dynamics simulations we investigate the properties of the *nonaffine* displacement field induced by macroscopic uniaxial deformation of amorphous silica, a strong glass according to Angell's classification. We demonstrate the existence of a length scale ξ characterizing the correlations of this field (corresponding to a volume of about 1000 atoms), and compare its structure to the one observed in a standard fragile model glass. The "boson-peak" anomaly of the density of states can be traced back in both cases to elastic inhomogeneities on wavelengths smaller than ξ where classical continuum elasticity becomes simply unapplicable.

DOI: [10.1103/PhysRevLett.97.055501](https://doi.org/10.1103/PhysRevLett.97.055501)

PACS numbers: 61.43.Fs, 46.25.-y, 62.20.Dc, 63.50.+x

The vibrational dynamics of glasses and, in particular, the vibrational anomaly known as the "Boson peak", i.e., an excess of the low-energy density of state in glasses relative to the Debye model, have attracted considerable attention in condensed matter physics [1–3]. This anomaly is observed in Raman and Brillouin spectroscopy [4,5] and inelastic neutron scattering [6] experiments in many different systems (polymer glasses [7], silica [8], metallic glasses [9]) and the corresponding excitations are often associated with heat capacity or heat conductivity low temperature anomalies. Many interpretations of these vibrational anomalies have been put forward, and generally involve some kind of disorder generated inhomogeneous behavior [1], whose exact nature, however, is the subject of a lively debate [2–5,10]. One related question is the possibility to determine a characteristic length in the vibration modes responsible for the Boson peak in glasses [5].

In this work, we argue that the natural origin of the vibrational anomalies in "fragile" as well as "strong" glasses lies in the inhomogeneities of the elastic response at small scales, which can be characterized through the correlation length ξ of the inhomogeneous or "*nonaffine*" part of the displacement field generated in response to an elastic deformation imposed at the macroscopic scale. The existence of such a length has been suggested in a series of previous numerical studies [11–13] on two and three dimensional Lennard-Jones (LJ) systems, and is experimentally demonstrated in macroscopic amorphous solids (foams [14], emulsions [15], granulars [16], etc.). At a more microscopic level, evidence has been provided recently by UV Brillouin scattering experiments on amorphous silica [17]. Being a natural consequence of the disorder of microscopic interactions [12] the nonaffine displacement field is responsible, in particular, for the breakdown of Born-Huang's formulation [18] for the prediction of elastic moduli [11,19,20], and has recently been studied theoretically by Lemaître *et al.* [20] and DiDonna *et al.* [21].

In practice, however, it appears that the only practical way to quantify this effect for a given material consists in direct molecular simulations [11,12]. The present contribution extends, for the first time, the numerical analysis to a realistic model of an amorphous silica melt—a strong glass according to Angell's classification [22]. Our results are compared to a previously studied fragile reference glass formed by weakly polydisperse LJ particles in 3D [13]. Strong and fragile systems have very different molecular organization and bonding. Although the intensity of vibrational anomalies is less important in fragile systems, it is well documented in experiments [7] on polymer glasses or in simulations of Lennard-Jones systems [23]. The observation of common features points to a universal framework for the description of low frequency vibrations in glassy systems. One recent finding of particular interest is that, in these LJ systems, the Boson-peak anomaly appears to be located at the *edge* of the nonaffine displacement regime, its position given by the frequency associated with ξ [12]. This begs the question whether this is a *generic* result applying also to other glasses, specifically to strong glass forming materials such as amorphous silica, which is characterized by an intricate local packing [23]—believed widely to be the *specific* origin of the vibrational anomaly [2]. As in our earlier contributions, we will focus on the analysis of the nonaffine displacement field obtained in the *linear elastic* strain regime and the eigenmode density of states for systems at zero temperature or well below the glass transition.

The amorphous silica was modeled using the force field proposed by van Beest *et al.* [24]. (For details about this "van Beest–Kramer–van Santen (BKS)" potential; see Refs. [25].) We performed classical *NVT* molecular dynamics simulations of systems containing $N = 8016$, 24 048, and 42 000 atoms with density $\rho = 2.37 \text{ g/cm}^3$, in fully periodic cubic cells with sizes $L = 48.3$, 69.6, and 83.8 Å, respectively. The short ranged part of the BKS potential was truncated and shifted at a distance of 5.5 Å.

For the Coulomb part we used the Ewald method with a real-space sum truncated and shifted at 9 Å [26]. To obtain the silica glass, we first equilibrated all systems at $T = 5000$ K during 0.8 ns. An ensemble of three independent configurations was studied for each system size [27]. Next, we performed a quench from $T = 5000$ K to $T = 0$ K by decreasing linearly the temperature of the external heat bath with a quench rate of 1.8 K/ps [25]. Finally, a conjugate gradient algorithm was used to minimize the potential energy of the systems yielding $T = 0$ K configurations with hydrostatic pressure $\langle P \rangle \approx 0.4$ GPa. The static properties were checked against published results obtained with the same amorphous silica model [25].

We now describe briefly the protocol used in order to investigate the elastic behavior at zero temperature of the model glasses under uniaxial deformation (for more details, see Refs. [11,12]). The procedure consists of applying a global deformation of strain $\|\epsilon_{xx}\| \ll 1$ to the sample by rescaling all coordinates in an *affine* manner. Starting from this affinely deformed configuration, the system is relaxed to the nearest energy minimum, keeping the shape of the simulation box constant. The relaxation step releases about half of the elastic energy of the initial affine deformation and results in the displacement $\delta u(r)$ of the atoms relative to the affinely deformed state, defining the nonaffine displacement field. A typical field for a silica glass is presented in Fig. 1, where a 2D projection of $\delta u(r)$ in the plane containing the applied deformation direction is shown.



FIG. 1. Inhomogeneous part $\delta u(r)$ of the displacement field $u(r)$ for the imposed macroscopic uniaxial strain in elongation $\epsilon_{xx} = 5 \times 10^{-3}$ for a silica glass containing $N = 42000$ particles ($L = 83.8$ Å). Projection of the field is done on the $(x-z)$ plane for all particles with position r close to the plane. The arrow length is proportional to $\delta u(r)$ and scaled by a factor of 150. The field resides in the linear elastic regime, i.e., has a magnitude varying linearly and reversibly with the applied deformation. As visual inspection shows, it is strongly spatially correlated and involves a substantial fraction of all atoms.

This procedure allows us to measure directly the elastic coefficients from Hooke's law [11], i.e., from the stress differences $\Delta\sigma_{\alpha\beta} = \sigma_{\alpha\beta}^{\text{end}} - \sigma_{\alpha\beta}^{\text{ref}}$, $\sigma_{\alpha\beta}^{\text{ref}}$ being the total stress tensor of the reference state configuration (quenched stresses), and $\sigma_{\alpha\beta}^{\text{end}}$ the one measured in the deformed configuration after relaxation. From the resulting values of the Lamé coefficients $\lambda = \Delta\sigma_{yy}/\epsilon_{xx}$ and $\mu = (\Delta\sigma_{xx} - \Delta\sigma_{yy})/2\epsilon_{xx}$ one obtains the associated transverse and longitudinal sound wave velocities, $C_T = \sqrt{\mu/\rho}$, $C_L = \sqrt{(\lambda + 2\mu)/\rho}$. In the case of the silica glass ($\lambda \approx 34.4$ GPa, $\mu \approx 37.2$ GPa, $C_T \approx 3961.4$ m/s, $C_L \approx 6774.5$ m/s), these quantities are in good agreement with data from Horbach *et al.* [25] and Zha *et al.* [28] (for silica under a density of 2.2 g/cm³, taking into account the scaling factor $(2.37/2.2)^{1/2}$ [25] inherent to the choice of a higher density).

The *linearity* of the strain dependence of both the displacement field and the stress difference $\Delta\sigma_{\alpha\alpha}$ have been verified explicitly following Ref. [12]. The *elastic* (reversible) character of the applied deformation is checked by computing the remaining residual displacement field after removing the external strain [12]. An alternative quantification of the plastic deformation is obtained by considering the participation ratio $\text{Pr} = N^{-1}(\sum_i \delta u_i^2)^2 / \sum_i (\delta u_i^2)^2$ of the noise $\delta u(r)$ [12]. As long as $\text{Pr} \approx 1$, all atoms are involved in the nonaffine field, while irreversible plastic rearrangements are marked by $\text{Pr} \rightarrow 0$, with only a few particles involved. A choice of $\epsilon_{xx} = 10^{-7}$ for the LJ glass with $L = 56\sigma$ and of $\epsilon_{xx} = 5 \cdot 10^{-3}$ for the silica glass were found to ensure *reversible and linear* behavior, with $20\% < \text{Pr} < 30\%$ and $25\% < \text{Pr} < 40\%$, respectively [29].

Visual inspection of the snapshot suggests that the field is strongly correlated over large distances, with the presence of rotational structures previously observed in Ref. [12] for LJ systems [30]. In order to characterize this kind of structure, we normalize the field by its second moment, i.e. $\delta u(r) \mapsto \delta u(r) / (\delta u(r)^2)^{1/2}$. In this way, in the linear elastic regime, it becomes independent of the applied strain and the system size [21].

Next, we study the Fourier power spectrum of the fluctuations of this normalized field. This spectrum can be described by two structure factors, $S_L(k) \equiv \langle \|\sum_{j=1}^N \underline{k} \cdot \delta u(r_j) \exp(i\underline{k} \cdot r_j)\|^2 \rangle / N$ relative to the longitudinal and $S_T(k) \equiv \langle \|\sum_{j=1}^N \underline{k} \wedge \delta u(r_j) \exp(i\underline{k} \cdot r_j)\|^2 \rangle / N$ relative to the transverse field component [12]. These quantities are plotted in Fig. 2 as a function of the wavelength $\lambda = 2\pi/k$, where $\underline{k} = k\hat{k} = (2\pi/L)(l, m, n)$ with \hat{k} being the normalized wave vector. Brackets $\langle \cdot \rangle$ denote an average over the degeneracy set associated with λ , and over an ensemble of configurations. As expected from our study of LJ glasses [12], the longitudinal power spectrum of silica is always smaller than the transverse one. The main difference between the two materials resides in the *hierarchical progression* of the decoupling between transverse and longitudinal contributions at short wavelengths

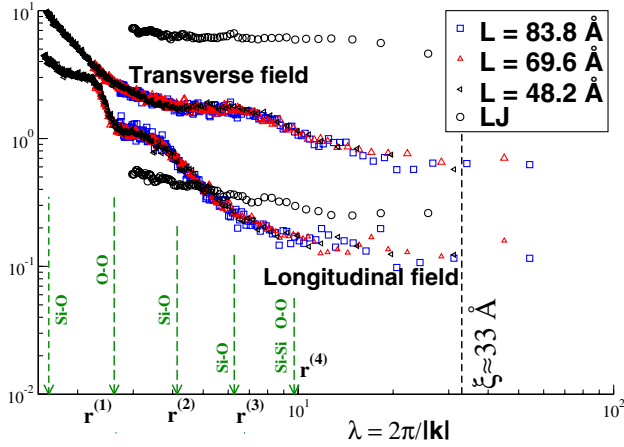


FIG. 2 (color online). Squared amplitudes of the quantities $S_L(k)$ and $S_T(k)$ (see text) for the longitudinal (bottom) and transverse contributions to the *normalized* nonaffine field $\delta u(r)$ of silica glass at $T = 0$ K under macroscopic elongation, plotted vs the wavelength $\lambda = 2\pi/k$ (in Å). The various system sizes included demonstrate a perfect data collapse. The transverse contribution is more important for all wavelengths. The spectra become constant for large wavelengths with a relative amplitude of about 10. The spectra for a LJ glass (circles, wavelength given in beads diameters) have been included for comparison [31].

that appears in the case of the silica glass (the spectra of LJ systems being only weakly wavelength dependent). This can be traced back to the local structure of silica which is represented by arrows giving the positions of the n first neighbor shells $r_{\{\alpha-\beta\}}^{(n)}$, where $n \in [1, 4]$ and $(\alpha, \beta) \in \{\text{Si}, \text{O}\}$. Structural effects disappear at distances greater than 4–5 tetrahedral units SiO_4 , i.e. $r_{\{\alpha-\alpha\}}^{(4-5)}$ with $\alpha \in \{\text{Si}, \text{O}\}$, and the longitudinal contribution to the nonaffine displacement field becomes then about 10 times smaller than the transverse one—similar to our finding for LJ systems [12,31].

We conclude that the nonaffine displacement field is of predominantly *rotational* nature in both fragile and strong glasses, and proceed to extract a characteristic length representative of this rotational structure. Considering the coarse-grained field $\underline{U}_j(b) \equiv N_j^{-1} \sum_{i \in V_j} \delta u(r_i)$ of all N_j particles contained within a cubic volume element V_j of linear size b , we compute the coarse-graining function $B(b) \equiv \langle \underline{U}_j(b)^2 \rangle_j^{1/2}$. As shown by Fig. 3, we find for *both* glasses an exponential decay, well fitted by the characteristic scales $\xi \approx 23\sigma$ for the fragile glass, and $\xi \approx 33$ Å, i.e., near $23 \times r_{\{\text{Si}-\text{O}\}}^{(1)}$ for the strong glass. The latter length scale has also been indicated in Fig. 2. The exponential behavior becomes more pronounced with increasing system size (not shown) which reduces the regime of the cutoff observed at large $b/L \approx 1$, which is expected from the symmetry of the total nonaffine field. [$B(b) \rightarrow 1$ for $b \rightarrow 0$ due to the normalization of the field.]

The existence of such a characteristic length scale has already been underlined in Ref. [12] for the LJ system, and

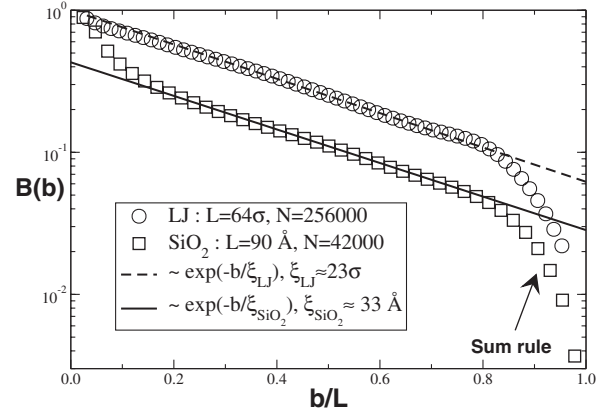


FIG. 3. Amplitude of the coarse-graining function $B(b)$ of the normalized nonaffine field averaged over a volume element of lateral size b , versus the ratio b/L , for LJ and silica (squares) systems under uniaxial elongation. Since the total displacement is zero by symmetry $B(b)$ must necessarily vanish for large $b \approx L$ (“sum rule”). For sufficiently large system sizes, which allow probing a broad $\sigma/L \ll b/L \ll 1$ region, our data demonstrates an exponential decay with characteristic length scale $\xi \approx 23\sigma$ for LJ and $\xi \approx 33$ Å for silica glasses.

has been related to the position of the Boson peak in the density of vibrational states. In order to test this assumption in the case of the silica glass, we computed the vibrational density of states (VDOS) $g(\nu)$ using the Fourier transform of the velocity autocorrelation function [25], calculated during 1.6 ns at $T = 300$ K (followed after a run of 8 ns to assure equipartition of the kinetic energy at this temperature). The VDOS is shown in the inset of the Fig. 4, and is in good agreement with results from Ref. [25]. In the main part of Fig. 4, reduced units $x = \nu \times \xi / C_T$ are used in order to plot the excess of vibrational states according to Debye’s continuum prediction, i.e. $g(x)/g_{\text{Debye}}(x)$, with ξ the previous characteristic length scales and C_T the sound velocities for transverse waves, for LJ and silica glasses. (The Debye prediction must obviously become correct for small eigenfrequencies. To access this frequency range even larger simulation boxes are needed.) This plot confirms the fact that the Boson-peak position can be well approximated by the frequency associated with the correlation length ξ of elastic heterogeneities in both LJ and silica glasses.

In summary, we have demonstrated the existence of inhomogeneous and mainly rotational rearrangements in the elastic response to a macroscopic deformation of amorphous silica. Our results are similar to the ones obtained previously for LJ glasses. The characterization of the non-affine displacement field demonstrates the existence of correlated displacements of about 1000 particles corresponding to elastic heterogeneities of characteristic size ξ of 20 interatomic distances. The estimate of the frequency associated with this length is in good agreement with the Boson-peak position. The existence of such a characteristic length in glasses should encourage to view

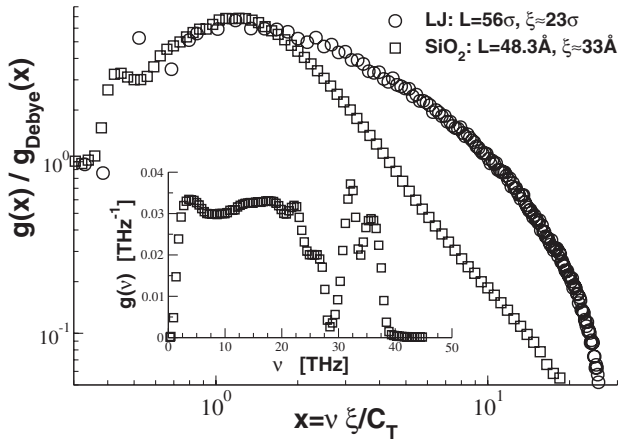


FIG. 4. Inset: VDOS $g(\nu)$ for the silica glass at $T = 300$ K. Main figure: Excess of vibrational states $g(x)$ compared to Debye's continuum model $g_{\text{Debye}}(x)$, using reduced units $x = \nu\xi/C_T$, with $C_T \approx 4.2$ (in LJ units) and $C_T \approx 3961.4$ m/s for LJ and silica, respectively, and ξ as indicated in the figure. The Boson-peak position at $x \approx 1$ is well approximated by the frequency associated with the wavelength of order ξ . As expected, the peak is more pronounced for the strong glass.

the Boson peak as a length—rather than a frequency—marking the crossover between a regime where vibrations in glasses with wavelengths larger than ξ can be well described by a classical continuum theory of elasticity, and a small wavelength regime where vibrations are strongly affected by elastic heterogeneities.

In a nutshell, the vibrational anomaly is therefore simply due to physics on scales where classical homogeneous continuum elastic theories (such as the Debye model) must necessarily break down. This leaves unanswered the important question what additional excitations are probed that produce the peak but suggests a similar description for different glass formers. Interestingly, the existence of a length scale of comparable magnitude accompanying the glass transition of liquids as been demonstrated very recently [10]. This (dynamical) length characterizes the number of atoms which have to move simultaneously to allow flow just as our (static) length ξ describes the correlated particle displacements. Since the glass structure is essentially frozen at the glass transition both correlations may be closely related, possibly such that the nonaffine displacements might be shown in future work to be reminiscent of the dynamical correlations at the glass transition.

Computer time was provided by IDRIS, CINES, and FLCHP.

- [1] See the reference lists of: V.L. Gurevich *et al.*, Phys. Rev. B **67**, 094203 (2003); J. Horbach *et al.*, Eur. Phys. J. B **19**, 531 (2001).
 [2] M. Foret *et al.*, Phys. Rev. B **66**, 024204 (2002); B. Rufflé *et al.*, Phys. Rev. Lett. **90**, 095502 (2003); E. Courtens *et al.*, J. Phys. Condens. Matter **15**, S1279 (2003).

- [3] G. Ruocco *et al.*, J. Phys. Condens. Matter **13**, 9141 (2001); O. Pilla *et al.*, Phys. Rev. Lett. **85**, 2136 (2000); P. Benassi *et al.*, Phys. Rev. Lett. **78**, 4670 (1997).
 [4] R. S. Krishnan, Proc. Indian Acad. Sci. A **37**, 377 (1953); M. Yamaguchi *et al.*, Physica (Amsterdam) **263B**, 258 (1999); B. Hehlen *et al.*, Phys. Rev. Lett. **84**, 5355 (2000).
 [5] B. Rufflé *et al.*, Phys. Rev. Lett. **96**, 045502 (2006); E. Courtens *et al.*, J. Phys. Condens. Matter **15**, S1279 (2003).
 [6] U. Buchenau *et al.*, Phys. Rev. Lett. **53**, 2316 (1984); M. T. Dove *et al.*, Phys. Rev. Lett. **78**, 1070 (1997); E. Duval *et al.*, J. Non-Cryst. Solids **235**, 203 (1998).
 [7] E. Duval *et al.*, Europhys. Lett. **63**, 778 (2003).
 [8] E. Duval *et al.*, Philos. Mag. **84**, 1433 (2004).
 [9] M. Arai *et al.*, Philos. Mag. B **79**, 1733 (1999).
 [10] L. Berthier *et al.*, Science **310**, 1797 (2005).
 [11] J.P. Wittmer *et al.*, Europhys. Lett. **57**, 423 (2002); A. Tanguy *et al.*, Phys. Rev. B **66**, 174205 (2002).
 [12] F. Léonforte *et al.*, Phys. Rev. B **72**, 224206 (2005).
 [13] A LJ pair potential $U_{ij}(r) = 4\epsilon((\sigma_{ij}/r)^{12} - (\sigma_{ij}/r)^6)$ for slightly polydisperse beads is used with σ_{ij} uniformly distributed between 0.8σ and 1.2σ . All LJ data presented in this Letter refer to at a fixed density $\rho\sigma^3 = 0.98$ corresponding to a hydrostatic pressure $\langle P \rangle \approx 0.2$ at zero temperature. See Ref. [12] for details concerning the simulation protocol.
 [14] G. Debrégeas *et al.*, Phys. Rev. Lett. **87**, 178305 (2001).
 [15] M. Falk and J. Langer, Phys. Rev. E **57**, 7192 (1998).
 [16] C. Goldenberg *et al.*, Phys. Rev. Lett. **96**, 168001 (2006); **96**, 189902 (2006).
 [17] G. Masciovecchio *et al.*, "Evidence for a New Nano-Scale Stress Correlation in Silica" (to be published).
 [18] K. Huang, Proc. R. Soc. A **203**, 178 (1950); M. Born and K. Huang, *Dynamical Theory of Crystal Lattices* (Clarendon Press, Oxford, 1954).
 [19] J.F. Lutsko, J. Appl. Phys. **65**, 2991 (1989).
 [20] A. Lemaître and C. Maloney, cond-mat/0410592.
 [21] B.A. DiDonna and T.C. Lubensky, Phys. Rev. E **72**, 066619 (2005).
 [22] C.A. Angell, Science **267**, 1924 (1995).
 [23] W. Kob and K. Binder, *Glassy Materials and Disordered Solids* (World Scientific Publishing, Singapore, 2005).
 [24] B. W. H. van Beest *et al.*, Phys. Rev. Lett. **64**, 1955 (1990).
 [25] K. Vollmayr, W. Kob, and K. Binder, Phys. Rev. B **54**, 15 808 (1996); J. Horbach, W. Kob, and K. Binder, J. Phys. Chem. B **103**, 4104 (1999).
 [26] We use the implementation in the LAMMPS code described in S.J. Plimpton, J. Comput. Phys. **117**, 1 (1995).
 [27] The sample to sample variations of all properties discussed in this study were found to be small. This is expected since all quantities are self-averaging and $\xi \approx 33 \text{ \AA} \ll L$.
 [28] C.-S. Zha *et al.*, Phys. Rev. B **50**, 13 105 (1994).
 [29] The linear elastic regime for amorphous silica is much broader (higher plasticity threshold).
 [30] The affine part of the displacement field, $\underline{\epsilon} \cdot \underline{r}$, depends trivially on the bead position within the simulation box. As may be seen from Fig. 1, the nonaffine part does not.
 [31] In the vicinity of $k = 1\xi$ the magnitude of the plotted function is expected to be of order $\rho\xi$, where ρ is the number density and ξ the correlation length of the field. This explains the difference in magnitude between the two systems.